HHS Public Access

Author manuscript

Nat Mater. Author manuscript; available in PMC 2017 April 10.

Published in final edited form as:

Nat Mater. 2017 February ; 16(2): 230–235. doi:10.1038/nmat4772.

Single-platelet nanomechanics measured by high-throughput cytometry

David R. Myers[1,2,3,4,5], **Yongzhi Qiu**[1,2,3,4,5], **Meredith E. Fay**[1,2,3,4,5], **Michael Tennenbaum**[6], **Daniel Chester**[7,8], **Jonas Cuadrado**[6], **Yumiko Sakurai**[1,2,3,4,5], **Jong Baek**[1,2,3,4,5], **Reginald Tran**[1,2,3,4,5], **Jordan Ciciliano**[1,2,3,4,5], **Byungwook Ahn**[1,2,3,4,5], **Robert Mannino**[1,2,3,4,5], **Silvia Bunting**[9], **Carolyn Bennett**[1], **Michael Briones**[1], **Alberto Fernandez-Nieves**[4,6], **Michael L. Smith**[10], **Ashley C. Brown**[7,8], **Todd Sulchek**[11], and **Wilbur A. Lam**[1,2,3,4,5]

[1]Department of Pediatrics, Division of Pediatric Hematology/Oncology, Aflac Cancer Center and Blood Disorders Service of Children's Healthcare of Atlanta, Emory University School of Medicine, Atlanta, GA 30322

[2]The Wallace H. Coulter Department of Biomedical Engineering, Georgia Institute of Technology & Emory University, Atlanta, GA, 30332

[3]Winship Cancer Institute of Emory University, Atlanta, GA, 30322

[4]Parker H. Petit Institute of Bioengineering and Bioscience, Georgia Institute of Technology, Atlanta, GA 30332

[5]Institute for Electronics and Nanotechnology, Georgia Institute of Technology, Atlanta, GA 30332

[6]School of Physics, Georgia Institute of Technology, Atlanta, GA, 30332

[7]Joint Department of Biomedical Engineering, North Carolina State University and University of North Carolina at Chapel Hill, Raleigh, NC 27695

[8]Comparative Medicine Institute at North Carolina State University, Raleigh, NC 27695

[9]Department of Pathology, Emory University School of Medicine, Atlanta, GA 30322

[10]Department of Biomedical Engineering, Boston University, Boston, MA, 02215

[11]George W. Woodruff School of Mechanical Engineering, Georgia Institute of Technology, Atlanta, GA, 30332

Abstract

Corresponding Author: Wilbur A. Lam, Address: 2015 Uppergate Dr, NE; Emory Children's Center - Room 448; Atlanta, GA 30322, wilbur.lam@emory.edu, Phone: 404-727-7473, Fax: 404-727-4455.

Supplementary Information is linked to the online version of the paper

Author Contributions: DRM & WAL conceived of and designed platelet contraction experiments. DRM, YQ, ACB, JC, BA, MS, TS, & WAL designed and tested platelet contraction cytometer. DRM, MT, DC, JC, YS, JB, RT, RM, SB, CB, MB, AFN performed experiments. MEF designed and wrote image analysis algorithms. DRM & WAL analyzed data and wrote the manuscript.

The authors declare no competing financial interests.

Haemostasis occurs at sites of vascular injury, where flowing blood forms a clot, a dynamic and heterogeneous fibrin-based biomaterial. Paramount in the clot's capability to stem haemorrhage are its changing mechanical properties, the major driver of which are the contractile forces exerted by platelets against the fibrin scaffold [1]. However, how platelets transduce microenvironmental cues to mediate contraction and alter clot mechanics is unknown. This is clinically relevant, as overly softened and stiffened clots are associated with bleeding [2] and thrombotic disorders [3]. Here, we report a high-throughput hydrogel based platelet-contraction cytometer that quantifies single-platelet contraction forces in different clot microenvironments. We also show that platelets, via the Rho/ROCK pathway, synergistically couple mechanical and biochemical inputs to mediate contraction. Moreover, highly contractile platelet subpopulations present in healthy controls are conspicuously absent in a subset of patients with undiagnosed bleeding disorders, and therefore may function as a clinical diagnostic biophysical biomarker.

During clot formation, various physiological cues such as damaged blood vessels or shear forces initiate platelet activation, adhesion, and the coagulation cascade, which lead to fibrin polymerization. Activated platelets then aggregate and bind to the nascent fibrin network via the $\alpha_{IIb}\beta_3$ integrin and undergo actomyosin-mediated muscle-like contraction (Supplementary Figure 1, Supplementary Video 1), which significantly decreases the overall clot size while increasing clot stiffness by several orders of magnitude. While this platelet-driven clot contraction has been well described in the literature, the mechanistic underpinnings and especially the biochemical and biophysical parameters that mediate this process remain poorly understood due to technological barriers. Current assays provide force measurements during clot contraction, establishing a link between average platelet force and different diseases [4], but these operate at the bulk level [1,3,5,6].

As recent studies demonstrate, microenvironmental cues such as mechanical properties of the underlying matrix substrate [7,8], matrix geometry [9], biochemical conditions [10], and shear stress [11,12] all mediate platelet physiology at the single cell level. In addition, clots in the hemodynamic environment are innately heterogeneous in which shear rate, fibrin architecture, and agonist concentration all vary significantly throughout the same clot. Therefore, a high-throughput, single platelet contraction assay is needed to establish and understand the "fundamental driver" of clot contraction, that is, how an individual platelet integrates biochemical and biophysical inputs to contract against the microenvironmental fibrin/ogen network. As fibrin mechanics have been well characterized, [13] deciphering this fundamental driver of clot contraction is the "missing link" needed to reconstruct higher order clot behavior and to obtain a comprehensive physical understanding of clot mechanics at multiple length scales.

To that end, we developed a microfabricated chip that simultaneously measures the contractile force of hundreds of individual platelets adherent on substrates with varied mechanical stiffnesses spanning the physiological range, while controlling the biochemical and shear microenvironment. This system overcomes technical barriers associated with existing techniques used for single cell analysis, such as the low throughput of atomic force microscopy [8]; the high computational needs of traction force microscopy [14]; or aggregate platelet measurements with micropillar arrays [15]. Here, an activated platelet adheres to and

spans a fibrinogen microdot pair and contracts the microdot pair together (Figure 1a–c, Supplementary Video 4). As contraction force is proportional to the fibrinogen microdot area and microdot displacement, relatively high-throughput measurements can be conducted with single cell resolution (Figure 1d–e), effectively creating a "platelet contraction cytometer." Imaging studies of the fibrin architecture in a developing clot informed microdot spacing/size (Supplementary Figure 1, Supplementary Information, and Methods: Optimizing plating), recapitulating the geometry of the *in vivo* platelet microenvironment. Since the platelet behavior of spanning and pulling microdots together is morphologically similar to clot behavior of platelets in fibrin meshes, trends observed in this system are expected to match those observed in a 3D system. Hydrogel stiffnesses of 5 – 100 kPa were used to approximate the range of mechanical environments encountered by a platelet within a clot (Supplementary Figure 2).

Because local biochemical agonists, hemodynamics, and mechanical properties of the clot directly mediate platelet physiology, we further refined our microfluidic system to enable encapsulation of micropatterned hydrogels of different stiffnesses in adjacent microchannels, enabling simultaneous testing of substrate stiffnesses, shear conditions, or agonist concentrations (Figure 2, Supplementary Figure 3). Each measurement of contraction force is not influenced by confounding effects such as the underlying substrate or neighboring platelet contraction, as shown by measurements of the gel thickness, stiffness, and microdot independence (Supplementary Figure 4). As thrombin, a potent physiologic platelet activator, and substrate stiffness both mediate different signaling pathways [7] that converge in clot contraction [16], the contraction cytometer was used to quantify how platelets synergistically integrate both biochemical and microenvironmental mechanical inputs to modulate contractile forces. Thrombin also converts fibrinogen to monomeric fibrin, enabling the experiments to more closely resemble the *in vivo* clotting environment [17,18].

Platelets have a highly nonlinear force curve (Figure 3) with maximum "peak" contraction force at moderate substrate stiffness and thrombin concentration, both within the physiologic range found in clots. While the observation of a peak force is similar to myocytes [19], platelets are unique in that output force is both mediated and requires a biochemical and mechanical input. Surprisingly, platelet contraction force is independent of shear stress (Supplementary Figure 5). As measurements are obtained after initial adhesion in our protocol, this independence suggests that shear effects are most significant in the early phases of activation. Interestingly, at the highest tested thrombin concentrations (5U/mL) characteristic of prothrombotic conditions, the subset of low contractile force platelets increases, thereby lowering the average platelet force (Figure 3). In addition, at highest stiffness conditions, platelets contract at lower forces demonstrating that this phenomenon is not simply due to the sensitivity limit of our system (Supplementary Figure 6).

Mechanistically, we discovered that the substrate stiffness-mediated platelet contractile force is highly dependent on the Rho/ROCK pathway (Figure 4a). To elucidate the underlying mechanotransductive mechanisms of how clot stiffness mediates contraction force, we employed two pharmacologic inhibitors of myosin light chain phosphorylation, ML7 and Y276232, which inhibit Ca^{2+}/calmodulin-dependent myosin light chain kinase (MLCK) and Rho kinase (ROCK), respectively. In light of previous results showing that MLCK and not

ROCK is essential to mechanosensitive spreading [7], our results showing ROCK and not MLCK is essential to mechanosensitive contraction highlight that the MLCK and ROCK pathways serve complementary mechanosensing functions in platelets. Previous studies have shown that the Rho/ROCK pathway is upregulated in cells adhered onto stiff environments [20] (RhoA) and is associated with stress fiber formation [21] (ROCK). Consistent with this idea is the observation that actin polymerization weakly correlates with increasing platelet contractile force (Supplementary Figure 7). As the platelet is anucleate, our data also demonstrate that mechanosensitive contraction can occur in the absence of gene expression.

To determine whether these findings on single platelets are related to changes in the bulk material properties of a blood clot, we conducted ROCK-inhibition experiments using standard bulk clot contraction assays and bulk clot rheology. We observed that ROCK-inhibition impairs bulk clot contraction as compared to the untreated control clots (Figure 4b), whereas MLCK inhibition did not alter clot contraction (Figure 4c). Bulk clot oscillatory rheology experiments, which enabled the simultaneous measurements of storage and loss moduli as well as bulk tensile forces, revealed that while both control and ROCK-inhibited clots undergo a dramatic stiffening process during the course of the experiment (Figure 4d), the exerted tensile forces differed but only at later time points. Specifically, control and ROCK-inhibited clots apply similar forces during the beginning of clot formation (Figure 4e) when the measured storage and loss moduli are low (Figure 4d). Over time, as the clots stiffen (Figure 4d), ROCK-inhibited bulk clots begin to exert lower tensile forces (Figure 4e) and plateau while the control continues to increase over time. Taken together, these bulk clot contraction observations are consistent with our data on individual platelet contractile force. In soft environments, both ROCK-inhibited individual platelet forces and ROCK-inhibited bulk contraction forces are similar to matching controls in bulk and at the single platelet level. In stiff environments, however, both ROCK-inhibited individual platelet forces and ROCK-inhibited bulk contraction forces are substantially lower than matching controls. As changes in bulk contraction can be due to multiple reasons, including changes in fibrin or rates of platelet contraction, our ROCK-inhibition single platelet contraction data together with the bulk data suggest that platelet contractile force alone can mediate these changes in bulk material behavior of clots. Hence, our data on individual platelet behavior in varying microenvrionements is not only associated with bulk clot contraction but can even inform the mechanisms occurring in bulk. Interestingly, the storage and loss modulus are the same for both ROCK-inhibited and control (Figure 4d), which may be due to the fact that the storage modulus of a clot is a function of both the density of cross-linking points [22], as well as tensioning of loose fibrin fibers [23].

Since *in vitro* clot contraction impairment is associated with limiting the maximum force exerted by a platelet, we hypothesized that low contractile forces measured at the single platelet level are associated with clinical bleeding disorders. To that end, we first measured the platelets from patients with impaired cytoskeletal machinery, which were expected to have lower contractile forces. Compared to healthy controls, patients with defective actomyosin machinery such as those with Wiskott Aldrich (WAS) syndrome, which involve mutations of the actin-related WAS protein gene, or MYH9-related disorders (MYH9RD), which involve mutations of the non-muscle myosin IIA gene, lack highly contractile platelets. Blood from WAS and MYH9 patients exhibit impaired bulk clot retraction, [24,25]

but these studies could not definitively pinpoint specific dysfunction in platelet contraction [25]. In our system, platelets from these patients exhibited significantly lower contraction force compared to those from healthy individuals in both stiff (Figure 5a) and soft mechanical environments (Supplementary Figure 8). More specifically, in these patients, a larger platelet subpopulation exerts near zero contractile force on stiff environments than for healthy subjects - approximately 30% versus 6% of platelets. Our single platelet measurements suggest that in these disorders, the impaired clot retraction may be due to the inability of individual platelets to apply appropriate forces.

Diminished platelet contractile forces were also found in a subset of a small cohort of patients presenting with chronic bleeding symptoms but normal clinical hemostasis tests. Specifically, these individuals have either normal or low-normal laboratory values for complete blood count, coagulation screening tests, platelet function (via PFA-100 or platelet aggregometry), or von Willebrand disease panels (Supplementary Table 1, Supplementary Table 2). Interestingly, three of the five patients showed impaired platelet contractility on stiff gels (Figure 5a), with a notable platelet subpopulation with forces below 20nN. Our platelet contraction cytometer's capability to detect these previous undiagnosable patients with bleeding diatheses, independent of existing clinical tests of hemostasis, suggests it may be a new potential category of diagnostic to evaluate for platelet dysfunction.

As shown above, a key capability of platelet contraction cytometry is single cell resolution and the detection of different platelet subpopulations based on contractility, providing a more nuanced understanding of what influences clot stiffening. Currently used contraction assays measure only bulk platelet contractility and do not detect the low contractile subpopulation that potentially correlates with disease. Even amongst our healthy donors, average platelet contractile forces varied considerably. However, platelet contractility cytometry revealed subpopulations of highly contractile platelets (with peaks at 30 nN and higher), which is consistent amongst all healthy donors (Figure 5b). We also observed individuals both with highly variable and highly consistent platelet contraction at different points in time (Supplementary Figure 9), indicating that platelet contraction force might be affected by a number of different physiological conditions, but in aggregate, establish a range that is consistently higher than the subset of bleeding patients described above. Our test then represents an important step towards the goal of personalized medicine.

By precisely controlling the mechanical, chemical, and shear microenvironments, this work defines the fundamental driver of clot stiffening, thereby providing important insights into clot mechanics. Although further clinical studies are warranted, we believe that our work demonstrates the proof of concept principles showing that our platelet contraction cytometer has the potential for clinical translation. The platelet contractility cytometer presented herein entails a simple fabrication process and represents a key technological advance in rapid, high-throughput, single cell force analysis. Models linking microscale measurements to macroscale clot mechanics are now possible, where they were previously hindered by the inherent mechanical complexity of fibrin and the lack of data on how single platelets sense their microenvironment and apply force. Our data shows for the first time that trends observed in individually contracting platelets are mirrored by changes in the bulk material properties of clots. Moreover, single platelet contraction measurements inform how the

material properties of a nascent clot directly affect platelet contraction and vice-versa, a correlation not accomplished by bulk assays. Our data further suggests that platelet contraction cytometry has the potential to serve as a useful addition to existing clinical tests of platelet function, as platelet contraction does not correlate with the currently used biomarkers of platelet activation (Supplementary Figure 7). Our newfound understanding of how platelet actuation directly affects clot formation and mechanics can be used to guide diagnostic strategies for thrombosis and bleeding disorders. Similarly, our contraction data and findings of the involved mechanotransductive pathways (Rho/ROCK) inform the development of pharmacological agents aimed at optimizing clot stiffness. Finally, this reductionist assay could be used to provide insight into other physiologically common cell and fibrous matrix systems that are often used in tissue engineering [26].

Methods

Device design: Fabrication

The device relies on the use of commercially available materials such as thin rolls of PDMS and rapid fabrication techniques such as laser cutting to achieve fabrication times of less than 8 hours per batch of devices (Supplementary Figure 3).

Laser cut gel mold—The first layer of the device will hold the polymerized patterned polyacrylamide gels and serve as the base layer. A laser cutter (Universal Laser Systems, VLS 3.5) is used to pattern long rectangular holes (1 mm x 25 mm) into a pre-fabricated sheet of PDMS (Rogers HT6240-0.01″) (Supplementary Figure 3). The PDMS sheets are ultrasonically cleaned with successive solutions of diluted Alconox, DI water, and ethanol. The sheets along with 24×40 mm No. 1 coverslips (Fisher Scientific) are then treated with an O_2 plasma (Harrick Plasma, PDC-32G) and covalently bonded together. The bonding is greatly improved after an overnight heat treatment at 60 C.

Once bonded together, the combined PDMS and coverslip piece was silanized. After an O_2 plasma treatment, pieces were incubated in a 10% (3-Aminopropyl)trimethoxysilane (Sigma 281778)/90% Ethanol/0.01% Glacial acetic acid solution for 90 min at 60C. The pieces were then vigorously rinsed with 70%ETOH/30% DI water three times, then rinsed with DI water three times. To improve the PDMS flexibility and surface properties, the pieces were left in DI water for 1 hour at room temperature. The pieces were then incubated with a 2% glutaraldehyde solution at room temperature for 30 minutes, then rinsed with DI water, and dried with compressed nitrogen.

Ligand (fibrinogen) stamped coverslips and optimal concentration—Stamped coverslips (No 1.5, 18mm × 18mm) were prepared using the lift-off method as described previously [27] (Supplementary Figure 3). The silicon mold to create the fibrinogen microdots was etched using standard lithography and etching techniques to a depth of 800 nm. Fibrinogen conjugated to AlexaFluor 488, 594, or 647 (Thermo Fisher Scientific) was used depending on other selected fluorophores in the experiment. The fibrinogen was incubated on10 mm x 10 mm x 3 mm PDMS squares at 30 μg/mL for 1 hour, rinsed off, and dried with compressed nitrogen. The PDMS squares with incubated fibrinogen were then brought in contact with O_2 treated silicon molds and removed to create a fibrinogen microdot pattern on

the PDMS. The microdot pattern was then transferred onto an O_2 plasma treated 18 mm x 18 mm coverslip.

Previous work has demonstrated that platelet spreading is greatly affected by the ligand density [28]. Surprisingly, platelet spreading is enhanced on low ligand density surfaces as compared with high ligand density surfaces. We attempted to both lower and increase the ligand density on our gels approximately 10 fold by changing the concentration of fibrinogen incubated on the PDMS stamps. For cases of low fibrinogen concentration on polyacrylamide gels, platelet adhesion was greatly diminished on the patterned surface, precluding contraction measurements. In cases of high fibrinogen concentration, the micropattern shape was often greatly deformed and of inconsistent brightness upon hydrogel polymerization. As such, our tests focused on concentrations of 30 μg/mL.

Polyacrylamide gel casting—To create wells for the polyacrylamide gel, the fibrinogen patterned coverslip was inverted and aligned over the hybrid 25 × 40 mm PDMS glass coverslip. This assembled piece was placed in an argon filled glovebox (MBraun UNIlab plus) after observing a 30 minute incubation under vacuum in the glovebox antechamber. In the glovebox, and directly prior to use, pre-mixed polyacrylamide solutions with appropriate ratios of acrylamide to bis-acrylamide in PBS, were mixed with N,N,N′,N′-Tetramethylethylenediamine (Sigma Aldrich, T9281), ammonium persulfate (Sigma Aldrich, A3678), and acrylic acid N-hydroxysuccinimide ester (Sigma, A8060) [29]. Using a 20 μL pipette, gel solutions were cast into the wells and allowed to polymerize for 90 minutes. Ammonium persulfate concentrations and NHS concentrations were optimized for an argon atmosphere and are approximately 10x lower than previously published values [29]. The concentrations used typically create a thin, unpolymerized region near the PDMS walls, ensuring that the hydrogel is mechanically isolated from the PDMS well. After polymerization, gels were removed from the glovebox and the 18 mm x 18 mm coverslip was removed and discarded. Gels were stored in PBS overnight and for up to seven days at 4°C.

Device Characterization—Fabrication of polyacrylamide gel-based systems have previously been shown to be highly controllable and repeatable [30] and previous experimental research [31] and subsequent mechanical models [32] determined that for polyacrylamide gels with thicknesses of >70 μm, the underlying glass substrate does not contribute to the locally measured stiffness. Here, the gels within our microdevice system are consistently >250 μm in thickness (Supplementary Figure 4), effectively preventing substrate effects from the underlying glass surface. We also performed atomic force microscopy measurements to determine the stiffness of the gel constructs. Measurements were performed on polyacrylamide gels in laser cut microchannels using a colloidal cantilever (sQube, CP-PNPL-PS-A) with a stiffness of 0.08 N/m and 1.98 μm diameter polystyrene sphere. Gel stiffnesses were in agreement with our calculated predicted values, and those reported by the literature [33] (Supplementary Figure 4).

Testing was performed to confirm that the microdot pairs are indeed independent of one another and that a contracting platelet does not affect the mechanics of the neighboring microdot pair. With this system, the displacement field around the applied point force is

expected decay over relatively short distances, as predicted by previous work [34]. Here, the microdot pairs are spaced far apart (8 μm or greater) relative to the microdot pair displacement caused by platelet contraction, which is on the order of 1 μm or less. At this distance, displacements induced by neighboring contracting platelets are expected to be negligible. To confirm this, we analyzed the microdot displacements of a single contracting platelet surrounded by empty microdot pairs in real time, and show that movement occurs only in the microdots to which the platelet is attached (Supplementary Figure 4). Some negligible movement may occur below the limit of detection of 0.05 μm, which was determined from measuring peak-to-peak movement in stationary microdots with no adherent platelets in the vicinity.

PDMS microfluidic top—PDMS microfluidics were cast from a SU-8 (Microchem Inc.) mold to create microfluidic channels and sized to cover the hydrogel strips. Microfluidics were 22 mm long x 1.5 mm wide, by 200 μm tall. To assemble, the gels were rinsed with DI water and dried to the extent that all water on the coverslip-PDMS piece was removed. This is greatly facilitated by the fact that the PDMS remains hydrophobic and the polyacrylamide gels are hydrophilic. The PDMS microfluidic was then quickly attached using a laser cut silicone adhesive (3M, 91022) to ensure that the gels do not dry during assembly. PBS was then flown into the enclosed channels until it was ready for use. The double sided tape approach is unique in that it provides rapid attachment of a microfluidic without affecting the patterned proteins.

Coverslip hybrid microfluidic top—The PDMS microfluidics were best suited to experiments requiring the use of shear flow. For experiments involving static flow conditions, a hybrid lid composed of laser cut PDMS and a coverslip facilitated imaging. Similar to conditions outlined above, premade PDMS sheets (Rogers HT6240-0.01″) were laser cut with well patterns, cleaned, and bonded to 18 mm x 18 mm No 1. glass coverslips. Using the same procedure outline in the PDMS microfluidic top, the coverglass and PDMS hybrid lid is bonded to the hydrogel device layer using laser cut silicone adhesive. Upon experimental completion, the ends of the device may be sealed with silicone grease for multi-day storage.

Experimental Methods

Platelet preparation—Healthy blood donors and patient donors had abstained from aspirin in the last two weeks, and consent was obtained according to GT IRB H15258. Blood was drawn by median venipuncture into acid-citrate-dextrose (ACD) solution 2. The sample was subsequently centrifuged at 150 G for 15 min, and the resulting platelet rich plasma was gel filtered into HEPES modified Tyrodes buffer as described previously [35]. Platelets were diluted to a final concentration of 4×10^6/mL in Tyrodes buffer to minimize potential paracrine signaling. This equated to an average distance between microdot pairs of 30–50 microns depending on the donor. In some experiments, platelets were incubated for 1 hour with vehicle (dimethyl sulfoxide, DMSO); ROCK inhibitor Y-27632 at 50 μm (Sigma Y0503), or MLCK inhibitor at 10 μm (Sigma I2764).

For bulk contraction studies, blood was drawn by median antecubital venipuncture into acid-citrate-dextrose (ACD) solution 2. The sample was centrifuged 150 G for 15 min and the resulting platelet rich plasma was collected, and centrifuged with an additional 10% ACD by volume at 900G for 5min. The supernatant, platelet poor plasma, was discarded and the platelets were resuspended into HEPES modified Tyrodes buffer.

Microdevice plating—Immediately prior to loading platelets into the microfluidic the following was added: 5 mM of $CaCl_2$, 5 mM of $MgCl_2$, 3 μg/mL of fibrinogen, thrombin (Haematologic Technologies, Inc), and any relevant inhibitors. The small dimensions of the microfluifidic ensure that platelets rapidly move to the ligand interaction region after activation. After 15 minutes, 60 uL of a wash solution consisting of 5 mM of $CaCl_2$, 5 mM of $MgCl_2$, thrombin, and any relevant inhibitors was used to remove residual platelets from solution. Thrombin both activates the platelets and converts microdot fibrinogen into monomeric fibrin, more closely recapitulating the in vivo environment [17,18]. For some experiment involving shear stress, flow was applied using syringe pumps (PhD Ultra, Harvard Apparatus) with the wash solution to create a shear rates of either $500s^{-1}$ or $1000s^{-1}$. The adhered platelets were then incubated for 90 minutes, which is several times more than needed for contraction to ensure that all platelets had sufficient time to reach a final state of contraction. Platelets were then fixed with a solution of Tyrodes buffer with 4% paraformaldehyde, 5 mM $CaCl_2$, and 5 mM $MgCl_2$ for 15 minutes.

Coverslip preparation & plating—In conditions where a platelet sample was extremely rare (WAS, MYH9-RD), was imaged live, or required later mounting for high resolution imaging, micropatterned gels on 25 mm coverslips were used. Bottom coverslips were prepared by silanized using the method described above, and top coverslips were micropatterned using the technique described above. Gels were then prepared and placed in between the coverslips. Similar plating protocols were used, with the exception that gel coverslips were placed in 6 well plates, and platelet concentrations were dropped to 2M/mL.

Plating optimization—Platelet behavior is affected by many different behaviors paracrine signaling, ligand density [28], ligand type, and shear stress [11]. The device presented in this paper sought to quantify changes in platelet contraction due to differences in substrate stiffness and thrombin concentration, while holding all other parameters constant.

ADP: Our initial experiments examining the effect of ADP on platelet contraction were inconsistent for the same individuals and over time. Measured forces were much lower than thrombin, but were extremely varied in both platelet adhesion and forces.

Platelet Concentration: Platelet behavior may be affected by nearby activated platelets. To minimize potential confounding effects, the platelet concentration chosen is purposefully low to ensure an average distance between contracting platelets of approximately 30 to 50 microns. There may be some enhancement of platelet contraction by neighboring platelets, but early tests with and without apyrase found no change in contraction measurements from the presence of apyrase.

Ligand Density: It is possible that order of magnitude changes in ligand density could affect outside-in signaling, as shown earlier [7,28]. We sought to examine this phenomenon but were constrained by the range of ligand densities that can be achieved using this system. Here, 30 μg/mL was optimal, creating well defined, repeatable patterns which supported platelet adhesion. When the stamping solution was 3 μg/mL, platelet adhesion was poor. At 300 μg/mL, the fibrinogen formed sheets which had the propensity to curl, lowering pattern fidelity. Overall, we expect trends presented here to be preserved on different ligand densities in light of previous reports [7] showing mechanosensitive trends are similar in low and high ligand density environments.

Shear Stress: Platelets were incubated for 15 minutes with thrombin concentrations of 0.1 or 1 U/mL on the polyacrylamide gels to ensure adhesion. Shear rates of 500 and 1000 s^{-1} applied for 1.5 hours to each thrombin concentration. Platelets were then fixed under flow with 4% PFA and imaged. No statistically significant differences were observed due to the application of shear stress from static controls at either thrombin concentration. Activating the platelets and allowing them to adhere to the fibrinogen under flow would enable shear stress to be applied during the entire activation process, leading to more firm conclusions that shear does not affect platelet contraction on fibrinogen with thrombin. Unfortunately, this condition is difficult to test as the constant flow of platelets also leads to multi-platelet aggregates.

Immunocytochemistry—After fixation, depending on the experiment, platelets were stained with an appropriate plasma membrane dye (Cell Mask Deep Red or Cell Mask Orange, Life Technologies). In some instances, platelets were counterstained with phallodin (Alexa Fluor conjugated, Life Technologies) or phosphatidylserine with Annexin V (Alexa Fluor conjugated, Life Technologies). For detecting activated $\alpha_{IIb}\beta_3$, FITC-PAC-1 antibody (BD Biosciences) was applied to platelets after 75 minutes.

Imaging & Mounting—Gels were imaged on a Zeiss LSM 700-405 confocal microscope using a 20x 0.8 NA lens. For high resolution images, samples were rinsed with DI water, inverted and mounted onto coverslips (ProLong Gold Antifade, ThermoFisher Scientific). High resolution images of platelets were obtained using a GE Deltavision OMX Blaze using a 100x, 1.49 NA objective.

For high resolution scanning electron microscopy, samples were extracted from microfluidics, and incubated overnight in 50% ionic liquid (IL1000, Hitachi) and 50% deionized water. Excess liquid was wicked away using filter paper. Samples were imaged using a Hitachi SU8230 cold field emission SEM.

Image Analysis—Images were analyzed using a MATLAB script which measured the fibrinogen microdot areas, and calculated the center to center distance of the fibrinogen microdots. Due to the high pattern fidelity, the initial uncontracted distance was taken to be the distance of a neighboring pair of uncontracted microdots. Although minimized, occasional multi-platelet aggregates identifiable by size occurred and were ignored. The current script and data collection is semi-automated, where confocal images are manually

collected, and individual platelet pairs are identified by hand, then subsequently analyzed by the script. Such a system may readily be adapted for automation in future studies.

Code Availability—The MATLAB script is freely available at GitHub (https://github.com/davidrmyers/platelet-contraction)

Bulk Isotonic Clot Contraction—Polystyrene fluorimeter cuvettes (Sigma-Aldrich) with attached grids of 1 mm spacing were incubated with 1% F-127 pluronic (Sigma) at room temperature for 1 hour. A solution consisting of 2 mg/mL of purified human fibrinogen (FIB 3, Enzyme Research Laboratories), and 250×10^6 washed platelets/mL was prepared. This platelet-fibrin solution was then combined with 1U/mL of thrombin and 5mM $CaCl_2$ in the cuvette and kept at room temperature. Pictures of clot contraction were taken every 30 minutes, and clot volume was estimated using the attached grid.

Bulk Isometric Rheology—Rheological measurements were performed with a stress-controlled rheometer (Anton Paar MCR 501) using cone-plate geometry. The clot was formed *in situ* and the shear moduli (G' and G'') as well as the normal force were measured as the clot formed. All measurements were done in the linear regime. Final clots composition consisted of: 2 mg/mL of purified human fibrinogen (FIB 3, Enzyme Research Laboratories), 250×10^6 washed platelets/mL, 1U/mL of thrombin, and 1 mM $CaCl_2$.

Supplementary Material

Refer to Web version on PubMed Central for supplementary material.

Acknowledgments

The authors wish to thank Andrew Shaw of the Parker H. Petit Institute for Bioengineering and Bioscience at the Georgia Institute of Technology (GT); Neil Anthony and the Emory University Integrated Cellular Imaging Microscopy Core of the Children's Pediatric Research Center; and the GT Institute for Electronics and Nanotechnology (IEN) cleanroom. Financial support provided by NIH R01 (HL121264), NIH U54 (HL112309), and NSF CAREER (1150235) to WAL; as well as an AHA Postdoctoral Fellowship to DRM. DRM thanks CRD and GAK for comments and discussion.

References

1. Jen CJ, McIntire LV. The structural properties and contractile force of a clot. Cell Motil. 1982; 2:445–55. [PubMed: 6891618]
2. HVAS & Sørensen. Tranexamic acid combined with recombinant factor VIII increases clot resistance to accelerated fibrinolysis in severe hemophilia A. 2007; doi: 10.1111/j.1538-7836.2007.02755.x
3. Collet JP, et al. Altered fibrin architecture is associated with hypofibrinolysis and premature coronary atherothrombosis. Arterioscler Thromb Vasc Biol. 2006; 26:2567–73. [PubMed: 16917107]
4. Carr ME. Development of platelet contractile force as a research and clinical measure of platelet function. Cell Biochem Biophys. 2003; 38:55–78. [PubMed: 12663942]
5. Cohen I, De Vries A. Platelet contractile regulation in an isometric system. Nature. 1973; 246:36–7. [PubMed: 4585844]
6. Young G, et al. Thrombin generation and whole blood viscoelastic assays in the management of hemophilia: current state of art and future perspectives. Blood. 2013; 121:1944–1950. [PubMed: 23319573]

7. Qiu Y, et al. Platelet mechanosensing of substrate stiffness during clot formation mediates adhesion, spreading, and activation. Proc Natl Acad Sci USA. 2014; 111:14430–5. [PubMed: 25246564]
8. Lam WA, et al. Mechanics and contraction dynamics of single platelets and implications for clot stiffening. Nat Mater. 2011; 10:61–6. [PubMed: 21131961]
9. Kita A, et al. Microenvironmental geometry guides platelet adhesion and spreading: a quantitative analysis at the single cell level. PLoS ONE. 2011; 6:e26437. [PubMed: 22028878]
10. Stalker TJ, et al. Hierarchical organization in the hemostatic response and its relationship to the platelet-signaling network. Blood. 2013; 121:1875–85. [PubMed: 23303817]
11. Nesbitt WS, et al. A shear gradient-dependent platelet aggregation mechanism drives thrombus formation. Nat Med. 2009; 15:665–73. [PubMed: 19465929]
12. Kroll MH, Hellums JD, McIntire LV, Schafer AI, Moake JL. Platelets and shear stress. Blood. 1996; 88:1525–41. [PubMed: 8781407]
13. Weisel JW. Biophysics. Enigmas of blood clot elasticity. Science. 2008; 320:456–7. [PubMed: 18436761]
14. Schwarz Henriques S, Sandmann R, Strate A, Köster S. Force field evolution during human blood platelet activation. Journal of cell science. 2012; 125:3914–20. [PubMed: 22582082]
15. Liang XM, Han SJ, Reems JAA, Gao D, Sniadecki NJ. Platelet retraction force measurements using flexible post force sensors. Lab Chip. 2010; 10:991–8. [PubMed: 20358105]
16. Suzuki-Inoue K, et al. Involvement of Src kinases and PLCgamma2 in clot retraction. Thromb Res. 2007; 120:251–8. [PubMed: 17055557]
17. Litvinov, RI., Gorkun, OV., Owen, SF., Shuman, H. Polymerization of fibrin: specificity, strength, and stability of knob-hole interactions studied at the single-molecule level. Blood. 2005. at <http://www.bloodjournal.org/content/106/9/2944.short>
18. Litvinov RI, et al. Polymerization of fibrin: direct observation and quantification of individual B: b knob-hole interactions. Blood. 2007; 109:130–138. [PubMed: 16940416]
19. Engler A, et al. Embryonic cardiomyocytes beat best on a matrix with heart-like elasticity: scar-like rigidity inhibits beating. J Cell Sci. 2008; 121:3794–802. [PubMed: 18957515]
20. Paszek MJ, et al. Tensional homeostasis and the malignant phenotype. Cancer Cell. 2005; 8:241–54. [PubMed: 16169468]
21. Burridge K, Wittchen E. The tension mounts: Stress fibers as force-generating mechanotransducers. The Journal of Cell Biology. 2013; 200:9–19. [PubMed: 23295347]
22. De Gennes, P-G. Scaling Concepts in Polymer Physics. Cornell University Press;
23. Shah J, Janmey P. Strain hardening of fibrin gels and plasma clots. Rheol Acta. 1997; 36:262–268.
24. Godwin H, Ginsburg D. May-Hegglin Anomaly: A Defect in Megakaryocyte Fragmentation? British Journal of Haematology. 1974; 26:117–127. [PubMed: 4853110]
25. Shcherbina A, et al. WASP plays a novel role in regulating platelet responses dependent on alphaIIbbeta3 integrin outside-in signalling. Br J Haematol. 2010; 148:416–27. [PubMed: 19863535]
26. Pedersen JA, Swartz MA. Mechanobiology in the third dimension. Ann Biomed Eng. 2005; 33:1469–90. [PubMed: 16341917]
27. Von Philipsborn AC, et al. Microcontact printing of axon guidance molecules for generation of graded patterns. Nat Protoc. 2006; 1:1322–8. [PubMed: 17406418]
28. Jirousková M, Jaiswal JK, Coller BS. Ligand density dramatically affects integrin alpha IIb beta 3-mediated platelet signaling and spreading. Blood. 2007; 109:5260–9. [PubMed: 17332246]
29. Polio SR, Rothenberg KE, Stamenović D, Smith ML. A micropatterning and image processing approach to simplify measurement of cellular traction forces. Acta Biomater. 2012; 8:82–8. [PubMed: 21884832]
30. Tse JR, Engler AJ. Stiffness gradients mimicking in vivo tissue variation regulate mesenchymal stem cell fate. PLoS ONE. 2011; 6:e15978. [PubMed: 21246050]
31. Engler AJ, Sen S, Sweeney HL, Discher DE. Matrix elasticity directs stem cell lineage specification. Cell. 2006; 126:677–89. [PubMed: 16923388]

32. Maloney JM, Walton EB, Bruce CM, Van Vliet KJ. Influence of finite thickness and stiffness on cellular adhesion-induced deformation of compliant substrata. Phys Rev E Stat Nonlin Soft Matter Phys. 2008; 78:041923. [PubMed: 18999471]

33. Tse JR, Engler AJ. Preparation of hydrogel substrates with tunable mechanical properties. Curr Protoc Cell Biol. 2010; Chapter 10(Unit 10.16)

34. Sabass B, Gardel M, Waterman C, Schwarz U. High Resolution Traction Force Microscopy Based on Experimental and Computational Advances. Biophys J. 2008; 94:207–220. [PubMed: 17827246]

35. McCabe White, M., Jennings, LK. Platelet Protocols: Research and Clinical Laboratory Procedures. Academic Press;

36. Gersh KC, Nagaswami C, Weisel JW. Fibrin network structure and clot mechanical properties are altered by incorporation of erythrocytes. Thromb Haemost. 2009; 102:1169–75. [PubMed: 19967148]

37. Collet JPP, Shuman H, Ledger RE, Lee S, Weisel JW. The elasticity of an individual fibrin fiber in a clot. Proc Natl Acad Sci USA. 2005; 102:9133–7. [PubMed: 15967976]

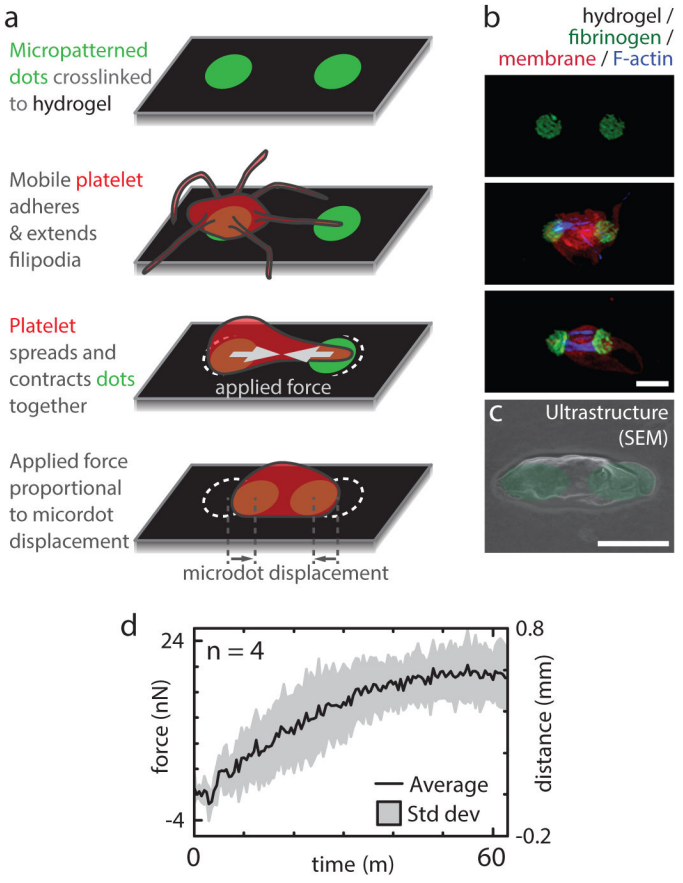

Figure 1.

The fundamental unit driving clot stiffening, a single platelet pulling against a fibrin/ogen substrate, is established by recapitulating the mechanical and biological microenvironment of the platelet. **a,** Fluorescently-conjugated fibrinogen microdot pairs are covalently bound to a deformable polyacrylamide hydrogel of known mechanical properties. As a platelet adheres and pulls pairs of fibrinogen microdots together, the contractile force is proportional to the microdot displacement. **b,** Super-resolution microscopy images of individual platelets with various degrees of contraction, scale bar is 2 μm **c,** Scanning electron microscopy image of a platelet contracting a fibrinogen microdot pair, scale bar is 2 μm. **d,** Real time contractile measurements of 4 single platelets.

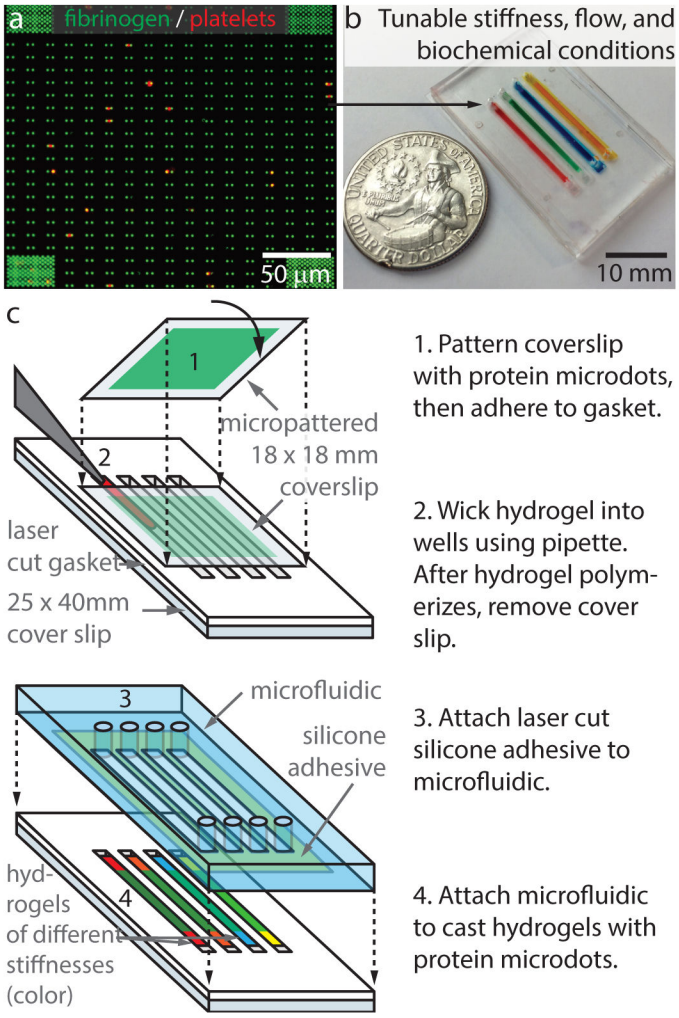

Figure 2.

Platelet contraction cytometer - hydrogels with microprinted arrays of fibrinogen microdots are encapsulated in separate microchannels, enabling the biochemical, mechanical, and shear microenvironments to be precisely controlled and varied simultaneously. **a,** A confocal image showing single platelets (red, contracting against fibrinogen microdot pairs (green) on the hydrogel surface. Over 20,000 fibrinogen microdot pairs are microprinted on the surface of each hydrogel encapsulated in each microchannel. **b,** Each microfluidic device may comprise different variables,, here four of microchannels comprise of hydrogels of different stiffness. **c,** A novel yet relatively simple fabrication process flow enables rapid manufacturing.

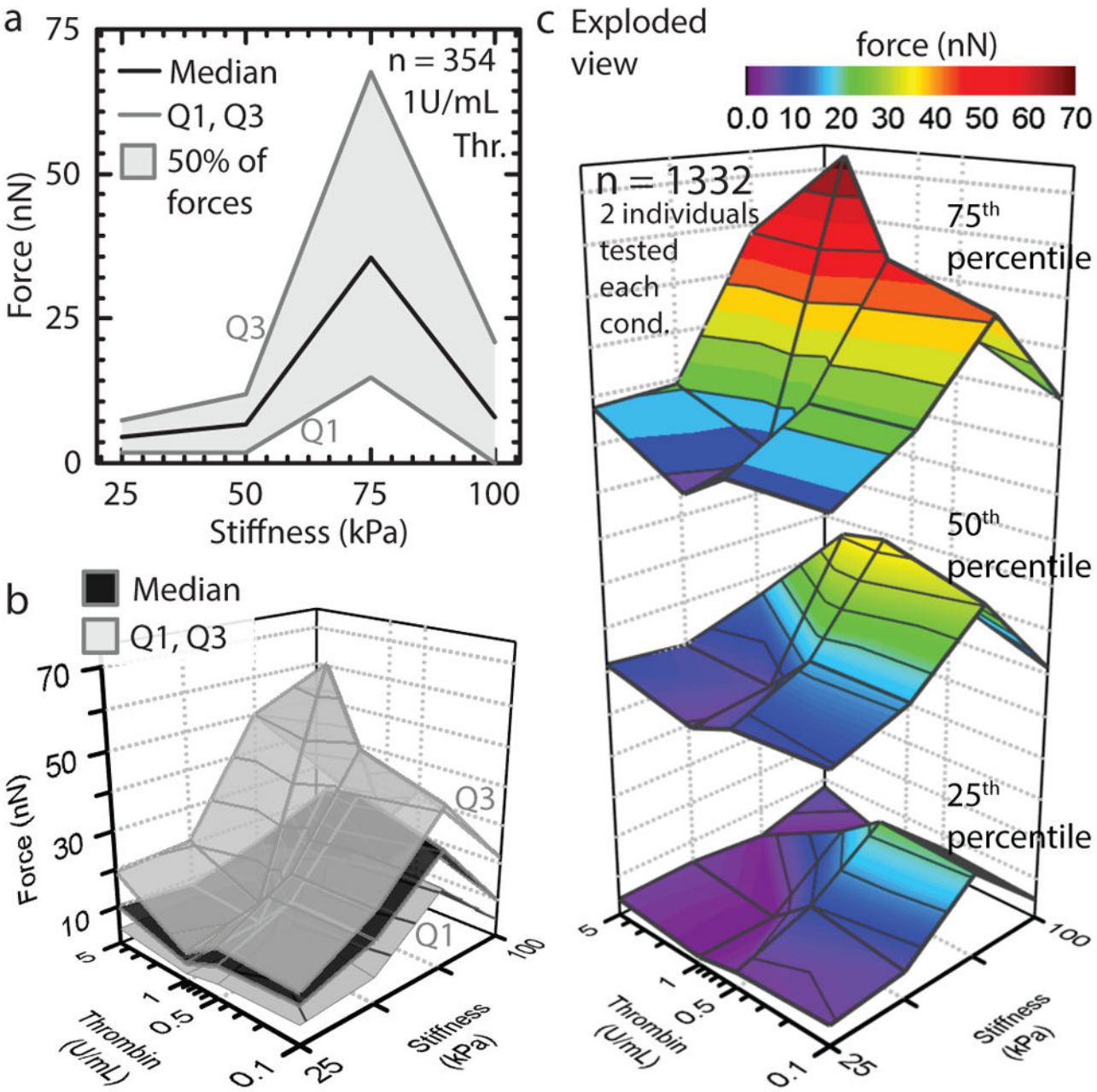

Figure 3.

Biochemical and mechanical cues synergistically mediate platelet contraction force. **a,** Maximal platelet contraction occurs at 75kpa substrate stiffness and 1U/mL thrombin. **b,** Single platelet force quartiles for physiologically relevant clot stiffnesses and thrombin concentrations. Platelet contractile forces are highest at a substrate stiffness of 75 kPa or at 5U/mL thrombin. A minimum occurs at 25 kPa stiffness and 1U/mL thrombin. **c,** Exploded view of b to aid visualization. Microenvironmental stiffness has a dominant role over thrombin concentration. Force attenuation at the highest stiffness conditions suggests a mechanically mediated negative feedback mechanism governing the upper limits of platelet contraction. n refers to total number of platelets tested.

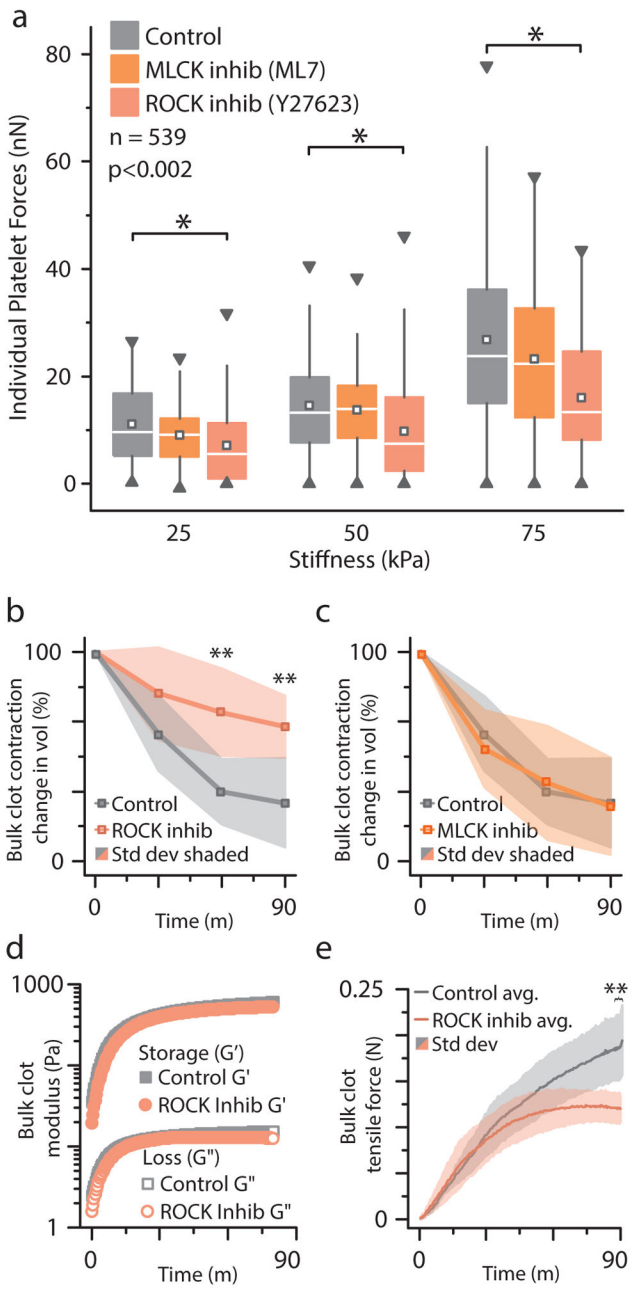

Figure 4.

Mechanotransductive platelet contraction is mediated by the Rho-associated protein kinase (ROCK) pathway, as measured with platelet contraction cytometry and standard bulk clot contraction and bulk clot rheology. **a,** The increase in platelet contractile forces with increasing substrate stiffness is significantly reduced with exposure to Y27623, a pharmacologic ROCK inhibitor. Pharmacologic inhibition of the myosin light chain kinase (MLCK) with ML7, on the other hand, did not produce a statistically significant difference in the substrate stiffness-mediated effect on platelet contractile force. Box denotes median and quartiles; whiskers to 1.5 interquartlie range), square denotes median, triangles denotes

1% and 99%. (n = 539, each condition n>40). * indicates differences from control at same stiffness ($p < 0.05$ by Mann-Whitney). **b,** ROCK inhibition impairs bulk clot contraction (n = 4) as compared to the untreated control clots. **c,** MLCK inhibition does not change bulk clot contraction (n = 4). **d,** Oscillatory rheology, which enables simultaneous measurements of storage (G') and loss (G'') moduli as well as bulk tensile forces, revealed that both control and ROCK-inhibited clots undergo a dramatic stiffening process (representative plot from 3 similar experiments shown). The angular frequency and strain amplitude are 1 rad/s and 0.01, respectively, which are well within the linear regime of the samples. **e,** Control and ROCK-inhibited clots apply similar forces during the beginning of clot formation when the measured storage and loss moduli are low (n = 3). As the clots stiffen (Figure 4d), ROCK-inhibited bulk clots begin to exert lower tensile forces and plateau while the control continues to increase over time. ** indicates difference from control ($p < 0.05$ by t-test).

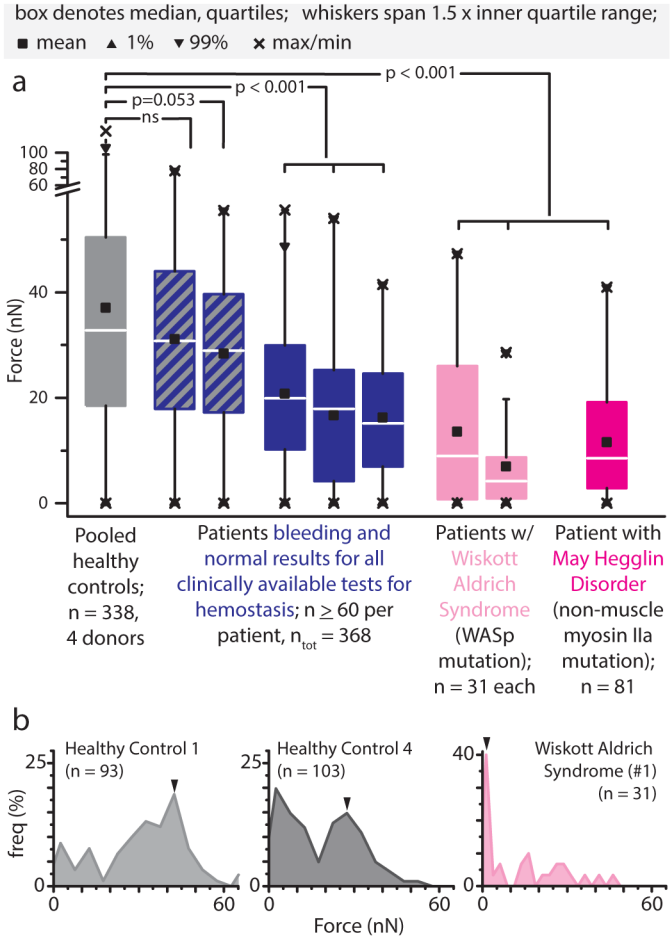

Figure 5.

Patients with phenotypic bleeding lack highly contractile platelets associated with clot contraction and force generation. **a,** Wiskott Aldrich Syndrome and May Hegglin Disorder platelets exhibited significantly reduced contractile forces compared to that of healthy controls (75 kPa gel stiffness, 1U/mL thrombin). In a subset of patients with bleeding diatheses yet normal hemostasis tests, platelet contraction was lower than that of normal healthy controls. **b,** Histogram data reveal platelet subpopulations of varying contractile forces. Healthy control platelets comprise high contractility subpopulations, notably absent in platelets from a Wiskott Aldrich Syndrome patient. In all panels, n refers to number of platelets, Mann-Whitney statistical test.